

Article

Thicknesses/Roughness Relationship in Mg-Al-Mg and Mg-Ti-Mg Hybrid Component Plates for Drilled Aeronautical Lightweight Parts

David Blanco , Eva María Rubio * , José Manuel Sáenz de Pipaón and Marta María Marín

Department of Manufacturing Engineering, Industrial Engineering School, Universidad Nacional de Educación a Distancia (UNED), St/Juan del Rosal 12, E28040 Madrid, Spain; dblanco78@alumno.uned.es (D.B.); jm@saenzdepipaon.com (J.M.S.d.P.); mmarin@ind.uned.es (M.M.M.)

* Correspondence: erubio@ind.uned.es; Tel.: +34-(91)-3988226

Received: 6 October 2020; Accepted: 17 November 2020; Published: 19 November 2020



Featured Application: Maintenance and repair drilling operations in aeronautic and aerospace sectors.

Abstract: Multimaterial hybrid compounds formed from lightweight structural materials have been acquiring great importance in recent years in the aeronautical and automotive sectors, where they are replacing traditional materials to reduce the mass of vehicles; this will enable either an increase in the action ratio or a reduction in the fuel consumption of vehicles and, in short, will lead to savings in transport costs and a reduction in polluting emissions. Besides, the implementation of production and consumption models based on the circular economy is becoming more and more important, where the repair and, for this purpose, the use of recyclable materials, is crucial. In this context, the analysis of a repair process is carried out by re-drilling Mg-Al-Mg multimaterial components using experimental design (DoE) based on Taguchi methodology, an analysis of variance (ANOVA) and descriptive statistics. The study concludes which are the significant factors and interactions of the process, comparing the results with previous similar studies, and establishing bases to determine the optimum thicknesses of hybrid magnesium-based component plates of drilled parts in the aeronautical industry, guaranteeing surface roughness requirements in repair and maintenance operations throughout their lifetime.

Keywords: hybrid components; light alloys; magnesium; aluminum; titanium; drilling; dry machining; sustainability; arithmetical mean roughness; repair and maintenance operations

1. Introduction

In Europe, there are approximately 448 airlines and 701 commercial airports that transported 606 million passengers during 2010 [1]. Air traffic has increased by a factor of 2.4 since 2000, and it was expected by pre-COVID-19 forecast an average increasing of 4.3% per year over the next 20 years [2]. Although the air transport sector has been strongly affected by the health crisis generated by the COVID-19, reducing the number of seats in 2020 by 50% [3], and the recovery of the sector will unfortunately not be immediate but expected between 2023 and 2025 [4], the long-term order forecast remains very important. For example, Boeing has a forecast of 48,400 aircraft by 2039 in October 2020, compared to 25,900 aircraft today [5], and the Airbus backlog stands at 7441 commercial aircraft at September 2020 compared to 7133 at the same point in last year [6], so efforts to optimize the sector's costs, and reduce fuel consumption and pollutant and greenhouse emissions, are still worthwhile.

The cost of fuel is estimated at 32% of the operating cost of Airlines [7]. Besides, commercial aviation is currently responsible for about 2% of global carbon emissions, and about 12% of all CO₂

emissions from the transport sector and, it is estimated that CO₂ emissions from commercial aircraft may triple by 2050, with air transport emissions reaching 25% of the total [8]. On the other hand, passenger cars, pickup trucks, vans, motorcycles, and other two- and three-wheeled vehicles constitute about one-third of the world's demand for petroleum. They generate about half of all transport-related greenhouse gas emissions, produce carbon monoxide, non-combusted hydrocarbons, sulphur oxides, nitrogen oxides, particles, and other air toxins [8] and, a total of 2 billion vehicles are expected by 2030 [9]. The European Union (EU) has a clear commitment to a gradual replacement of fossil fuels by renewable energies. In December 2018, the Renewable Energy Directive 2018/2001/EU entered into force, which sets a new binding target for renewable energy in the EU for 2030 of at least 32% to become the first climate-neutral continent by 2050 [10].

In 2018, all airlines in the world with international routes began to officially report their emissions as part of the Carbon Offsetting and Reduction Scheme for International Aviation (CORSIA), adopted by the United Nations in 2016, which aims to halve total carbon emissions by 2050 [11]. In June 2001, the Advisory Council for Aeronautics Research in Europe (ACARE) was created in Paris to develop and maintain a Strategic Research Agenda (SRA). This group consisted of the member states, the European Commission, and stakeholders from the aviation sector: the manufacturing industry, airlines, airports, service providers, regulators, research institutions, and academics. Among the goals defined for 2050 are a 75% reduction in CO₂ emissions per passenger and kilometer and a 90% reduction in NO_x emissions. Additionally, air vehicles must be designed and manufactured to be recyclable [1].

Within this framework, and to meet current and future requirements, new innovative materials, design techniques, and manufacturing processes are being developed to increase efficiency and reduce consumption [11]. The new families of Airbus aircraft are engineered to optimize fuel efficiency, the A320 and A350 aircraft save more than 20% in fuel consumption. The A350 includes more than 50% lightweight structural materials, and the A220's primary structure includes aluminum-lithium on the fuselage, and titanium and hybrid materials on the wings [12]. For its part, the Boeing 737 MAX family uses 20% less fuel than the aircraft it replaces, and it is as efficient as a hybrid electric car in terms of liters of fuel equivalent used per 100 km and passenger [13]. The priorities defined in Boeing's environmental policy are, firstly, the reduction of CO₂ emissions in all activities and, secondly, the optimization of fuel consumption [11].

There are different working lines to optimize consumption and reduce the emission of pollutants: the development of new engine technologies [9], the use of alternative technologies [12], and the reduction of the aircraft's weight, either by reducing their size or by replacing conventional heavy materials with new lightweight structural materials, or combinations of them while maintaining the same performance or improving it [14]. The present work is framed in this last working line.

The consensus regarding the benefit of mass reduction is clear and has been outlined in many studies. For each 100 kg of vehicle mass reduction, there is a reduction in fuel consumption of 0.38 L/100 km, and a reduction of 8.7 g of CO₂ per km [15]. Each kilogram of mass reduction produces a saving of 150,000 US dollars in fuel over the life of the engine [16]. A 10% reduction in the mass of a vehicle results in a reduction of fuel consumption of 5–7% [17]. One of the research and development lines currently open is based on the use of lightweight structural materials such as lightweight titanium, aluminum, and magnesium alloys, all with an excellent density/mechanical properties ratio [18–23], or plastic and polymer compounds [21,22]. For example, in the case of automotive vehicles, 40% of the total mass is in the car body; therefore, this is a key area for potential mass reduction [24]. On the other hand, it is fundamental to bear in mind that the recyclability of the materials selected for the design is a must from the very beginning. Over the next 20 years, more than 12,000 aircraft are expected to reach the end of their lifetime. Airbus has established a method for dismantling and recycling its aircraft parts, achieving 90% recycling or reuse and safe and sustainable disposal when recycling is not possible. Since 2007, Airbus has recycled 117 aircraft worldwide with 92% reuse of the remaining parts and 100% recycled engines [2,25].

Aluminum and magnesium are two of the most abundant materials on earth, and they have been widely studied separately, but the number of studies in which a multimaterial combination of them is machined is very limited. From a structural point of view, their main characteristic is an excellent density/mechanical resistance ratio [26]. This feature makes them very attractive when seeking to reduce mass to reduce fuel consumption and emissions while maintaining mechanical performance. In particular, aluminum alloys are the most commonly used lightweight structural materials and have been the subject of many scientific articles in recent years [21,22]. Moreover, Al and Mg alloys offer additional advantages such as their great capacity to be recycled [27,28] and their good machinability. However, they also present some common disadvantages such as lower mechanical resistance than other structural materials such as titanium or steel; lower working temperature; corrosion problems and worse weldability, among others [29]. On the other hand, titanium has very good mechanical, chemical, and thermal properties that complement those of magnesium and aluminum. It has a relatively low density, 4500 kg/m^3 so that the overall properties of the multimaterials in which titanium is combined maintain a good ratio between mechanical properties and density [29]. All this makes the study of possible combinations among these three light alloys in multimaterials, such as Mg-Al-Mg or Mg-Ti-Mg, very interesting for their potential applications in the reduction of the mass of vehicles and aircraft in a sustainable way.

Additionally, the current demands on high-performance parts make it difficult to design them using a single material. Therefore, it is often necessary to benefit from the properties of several materials to create a multimaterial or hybrid component with superior properties [30]. It is also feasible to develop new alloys with the required properties, but the process is long, and the target is not always achieved. For example, in the case of gamma alloys, the first commercial flight using alloy 4822 engines in Low-Pressure Turbine Blades (LPTBs) was conducted in March 2012, but the first exploratory research into gamma alloys had begun 40 years earlier [31]. Other interesting alloys under development included in recent studies are Ni-Al alloys with memory effect and superelasticity [32] and gamma alloys [31].

A topic of special interest within the hybrid components is the joining of dissimilar materials to create the multimaterial. The main joints are mechanical, through drilling and bolts or rivets [33], and thermal, through different welding technologies. The machining of multimaterial or hybrid composites in a single operation is a challenging task because of the different characteristics of the materials resulting in different optimal machining conditions. This requires the use of compromise solutions between tool geometry and cutting parameters and frequently results in severe tool wear, increased cutting forces, poor hole quality or large burrs, worsening the difficulties in the interface between materials [18,33–35]. For instance, the most common defects in drilling titanium in hybrid compounds are errors in hole size, roundness, position, and the existence of burrs. Titanium chips evacuation can cause scratches at the interface between materials and in the materials during the chip outlet, and the surface quality is also influenced by the number of holes made by the tool because of the effect of wear [33].

On the other hand, drilling plays a fundamental role in the assembly of parts in the aeronautical industry, and it is estimated to be used in 50% of the operations with chips removal. Therefore, it is frequently used in structural parts that require a subsequent assembly through bolts or rivets. The most frequent problems faced in the drilling process are high tool wear, poor surface quality, and out-of-tolerance diameter [36]. Likewise, a significant factor in the drilling process, analyzed in several recent works, is the influence of the tool geometry and/or its coating on the final quality of the process [7,20,33,37–39].

The manufacturing of parts of responsibility for industries such as aerospace or automotive requires very strict manufacturing tolerances in terms of dimensional, geometrical, and physical-chemical properties to ensure reliable and predictable behavior in service [40]. The usual range of roughness tolerances required in the aeronautical and aerospace sector in terms of arithmetical mean roughness, R_a (μm) is $0.8 \mu\text{m} < R_a < 1.6 \mu\text{m}$ [41]. In the case of rivets, they are repaired by drilling a hole to a

larger diameter and using either a larger diameter rivet or an ACRES[®] sleeve or similar which allows the use of a bolt of the nominal design diameter [42]. The metal sheets used in the aeronautical sector are mainly obtained by rolling, and their thickness most frequently varies from very thin sheets to sheet thicknesses of more than 6 mm [43].

In addition, the advantages of residual compression stress (RCS) generated by different manufacturing processes and its effect on improving the fatigue behavior of materials have been analyzed in various papers. For example, Barry et al. [44] carried out a study on the effect of shot peening on cast magnesium A8 parts. The researchers found that although the shot peening process significantly increases the surface roughness of the surfaces on which it is applied, the initiation of cracks on these surfaces is much lower than when it is not applied. The study concludes that the shot peening process increases fatigue life and delays the crack initiation, despite producing a significant increase in surface roughness. Besides, and within the study, it was achieved an increase of up to five times the working life and 30% of the fatigue resistance limit by applying shot peening to cast magnesium A8 parts. In UNS A92024-T3 aluminum alloys, studies have been carried out on the effect of compressive residual stress (CRS) generated by turning, concluding that the greater the residual compressive force generated, the greater the improvement in ultimate tensile strength (UTS) [45].

In addition, the use of cutting fluids reduces the friction between the tool and the chip, lubricates the tool–piece interface, dissipates the heat, and helps to remove the chip adhered to the tool surface [18,29]. However, it causes environmental and health damage from the chemical additives it contains. To avoid this, there is a tendency towards almost dry cutting formulas such as minimum quantity lubrication (MQL) [33,46] and dry machining [18–20,40,45], or new technologies such as cryogenic cooling [47]. These options provide new solutions for alloys such as titanium in which tool wear occurs due to its low thermal conductivity and high chemical affinity. However, working with extremely low temperatures produces a workpiece hardening and an increase in the cutting forces. Therefore, several studies have been recently published seeking solutions to this problem. In one of the studies, an internal cryogenic cooling for the tool that maintains the standard working temperature on the workpiece is used, reducing the cutting force by 54% and the tool wear by 90% compared to traditional cooling [48]. Other studies propose the use of an internal cryogenic cooling for the tool. In this direction, Pereira et al. [49] study the use of a cryogenic cooling with MQL lubrication that employs CO₂ as internal coolant, and Damir et al. propose a hybrid system of cryogenic and MQL which clearly improves cutting forces, surface quality, and tool life [50].

A requirement commonly used by manufacturers in the automotive and aerospace sectors as well as in numerous studies on light alloy machining is the Arithmetical Mean Roughness, R_a (μm) [18–20,40,46,51,52]. Therefore, R_a (μm) is the response variable chosen in this study to determine the optimum thickness of Mg-Al-Mg hybrid component plates for drilled parts in the aeronautical industry. Besides, it is used to compare the results with those obtained, in previous works, for other combinations of materials, Mg-Ti-Mg, of identical geometry.

Furthermore, the research method that modifies a factor in each test is very time-consuming and does not provide knowledge of the interactions between parameters. The design of experiments (DoE) is an experiment-based modeling method that uses statistical techniques, such as analysis of variance (ANOVA) to process the data and find out about the factors of influence, the interaction between them, and their level of influence on the process [18–20,51,53–56].

This study is part of a larger research project that includes several structural lightweight materials, machining processes, and lubrication/cooling systems. Two experimental tests were carried out in 2017, the first allowed to determine the factors with the greatest influence on the turning process in Al-Mg multimaterial specimens [19], the second studied the influence of the tool on the magnesium drilling process under different machining conditions on specimens [20]. In 2018, this knowledge was applied for the selection of the drilling tool for Mg-Ti-Mg multimaterial components in the search for the best dry machining parameters [18]. In 2019, a review of recent literature on hybrid composites was carried out which concluded that there is a clear scientific and automotive and aeronautical industry interest

in the use of aluminum alloys being the single most commonly used material to form multimaterial combinations [21]. Consequently, two experimental tests were carried out on Mg-Al-Mg multimaterial specimens to find the most significant factors in the process and the best machining conditions by applying sustainable cooling/lubrication techniques such as dry machining and cold compressed air. Besides, two different drill diameters were analyzed, finding slight differences depending on the diameter used, but the selection of influencing factors remained robust [57,58].

The novelty of this work is to carry out an analysis of magnesium-based multimaterial compounds focusing on the relationship between the thickness of the plates that form the compound and the multimaterial combination used. This analysis was carried out from a joint perspective and applying the previous knowledge acquired. Therefore, in addition to analyzing the data obtained in the individual experiment carried out for this study on a Mg-Al-Mg component, a comparative analysis was also carried out with the data obtained in a previous test framed in the same project and carried out on a Mg-Ti-Mg multimaterial combination [18]. The data from both studies are comparable because they follow the same methodological structure based on Taguchi [59], and designed for this purpose. The data from the previous study was reanalyzed following the perspective, objectives, and structure of the present study.

The study aims to establish the basis for correlating the surface quality obtained with the material combination of the hybrid magnesium-based components, the thicknesses of the plates that form them, and the cutting parameters in the repair and maintenance processes of drilled parts in the aeronautical industry so that the design requirements are guaranteed throughout their useful life. Furthermore, by carrying out tests with new materials, a complete table of materials, plate thicknesses, and the most suitable order of materials/drilling direction could be obtained, depending on the surface roughness required (as well as the cutting parameters under which this was achieved) so that it would serve as a guide in repair and maintenance operations to other researchers or workers in the topic. The ultimate goal is to use this new knowledge in applications involving the riveting of multimaterial plates made of light alloys in the aerospace industry.

An extensive review of recently published work on lightweight structural materials was conducted, in particular, those applied to the aeronautical and automotive sectors, in which sustainable manufacturing perspectives are applied. Moreover, following the Taguchi methodology on experimental design [59], a series of tests were designed and conducted, and the results analyzed through an analysis of variance to determine the effect of the significant factors and their interactions on the response variable, specifically the arithmetical mean roughness, $Ra(\mu\text{m})$.

Both types of specimens are geometrically identical and formed by hybrid magnesium-based compounds. Therefore, this comparative analysis can provide useful information to find potential constraints in the design of the current specimens and, subsequently, to redesign them so that future tests will provide more complete information on the process of repairing hybrid magnesium-based multimaterial by re-drilling.

From the analysis and comparison of both studies, the most favorable plate thicknesses found in the re-drilling process of the hybrid magnesium-based components are concluded, taking into account the materials that form the multimaterial. Besides, new thicknesses are proposed for the design of the specimens, and new tests will be carried out on both to verify the results, the current specimens, and the new specimens with the proposed thicknesses and settings.

2. Methodology and Materials

2.1. Methodology

This study is part of a research project that includes different lightweight structural materials, machining processes, and cooling/lubrication systems [18,19,57,58,60]. The methodology used is similar to the one followed in previous works in which the bases that provided the initial knowledge for this work were established. In previous studies within the same project, and using a similar

methodology to make the individual studies comparable, the influence factors on the turning of Mg-Al specimens were studied [19], the influence of the tool on the drilling of magnesium alloy parts was investigated [20], the best process parameters for re-drilling on titanium parts by dry machining were investigated to eliminate the use of lubricant/coolant fluids and thus make the process more sustainable and economical [18], and the parameters with the most influence on the re-drilling of hybrid multimaterial Mg-Al-Mg compounds with various re-drilling diameters were investigated [58,60]. This methodology is based on the Taguchi methodology and the Montgomery guidelines [59], to carry out a study in which the results can be compared with each other.

The methodology includes the following stages: pre-experimental planning in which the problem under study is defined, the identification of factors of influence, levels and ranges, and the choice of the response variable. Subsequently, the selection of the experimental design, its performance, and the statistical analysis of the results obtained takes place. Finally, after the discussion and the analysis of the results, the conclusions are drawn.

The problem under study is focused on repair and maintenance operations carried out by re-drilling on multimaterial or hybrid magnesium-based components, evaluating the cutting conditions and the sustainable cooling/lubrication techniques applied, and analyzing their influence on the results of the surface roughness obtained.

Since it is aimed at repair and maintenance operations, a single value of 0.5 mm was chosen for the depth of cut factor, *d*. Keeping the depth of cut at low values also helps to keep the cutting temperature low; being favorable to be far from the ignition temperatures of magnesium.

The type of cooling system, *C*, is a factor of great interest in the study of magnesium machining because of the special conditions that this material presents regarding ignition. For this reason, two levels were selected for the type of cooling, *C*, factor, the first level is Cold Compressed Air (CCA) and the second level is dry machining.

The cutting tool, which also has a great influence on the quality of the machining, was fixed on a 9 mm diameter high-performance twist drill. The test specimens consist of two magnesium plates with an aluminum plate in between. Chip evacuation was identified as a factor with potential influence, and, consequently, measurements of roughness were taken at the entrance and at the exit of each plate.

The following factors were established as factors of potential influence: the plate on which the measures are taken, Location Regarding Insert, *LRI*, and the position where the measures are taken on each plate, Location Regarding Specimen, *LRS*. The Location Regarding Insert factor has three levels depending on the plate *LRI1*: magnesium plate Mg1, *LRI2*: aluminum plate Al2 and *LRI3*: magnesium plate Mg3. The Location Regarding Specimen factor has two levels; depending on whether the measures are taken at the entrance of the hole, *LRS1*, or at the exit of the hole, *LRS2*.

For the feed per rev, *f* (mm/rev), and the spindle speed, *N* (r·min⁻¹), both factors with potential influence, two levels were set based on the previous experience of researchers in the machining of this type of multimaterials, *N*, 500/1200 and *f*, 0.05/0.1

Table 1 summarizes the factors used and the levels chosen for each factor.

Table 1. Factors and levels.

Factors	Levels (Code)	Levels (Values)	Type
Depth of cut, <i>d</i> , (mm)	<i>d1</i>	0.5	Quantitative
Feed rate, <i>f</i> (mm/rev)	<i>a1, a2</i>	0.05/0.1	Quantitative
Spindle speed <i>N</i> (rpm)	<i>N1, N2</i>	500/1200	Quantitative
Type of cooling system, <i>C</i>	<i>CCA, Dry</i>	<i>C1/C2</i>	Qualitative
Location Regarding Insert, <i>LRI</i>	<i>Mg1/Al2/Mg3</i>	<i>LRI1, LRI2, LRI3</i>	Qualitative
Location Regarding Specimen, <i>LRS</i>	Drill hole: entry/exit	<i>LRS1, LRS2</i>	Qualitative

The selected design was the product of a complete factorial 2³ and a block of two factors (3 × 2). Roughness values were taken at the entrance and exit of each hole in each of the three plates that conform the multimaterial, with a total of eight experimental re-drillings, and six *Ra* (µm) measurements

per hole, providing a total of 48 measurements that can be seen in Table 2. Roughness measurements were taken using a Mitutoyo SurfTest SJ 401 which has a measurement range of 800 μm and a resolution of 0.000125 μm and using the ISO-1997 standard.

Table 2. Mg-Al-Mg specimen experimental design: product of a full factorial 2³ and a block of two factors.

Test No.	1	2	3	4	5	6	7	8
LRI/LRS	LRI1/LRS1							
	LRI1/LRS2							
	LRI2/LRS1							
	LRI2/LRS2							
	LRI3/LRS1							
	LRI3/LRS2							
C	C1	C1	C1	C1	C2	C2	C2	C2
f (mm/rev)	f1	f1	f2	f2	f1	f1	f2	f2
N (rpm)	N1	N2	N1	N2	N1	N2	N1	N2

The areas where the roughness measurements are taken regarding the location of the plate within the hybrid compound, LRI factor, are LRI1 (Mg1), LRI2 (Al2), and LRI3 (Mg3), and the areas where roughness measurements are taken regarding its location within each hole, LRS factor, are LRS1 (entrance of the hole) and LRS2 (exit of the hole). Figure 1 shows a representation of the multimaterial component tested indicating the LRI factors on the left and the LRS factors on the right together with the drilling direction.

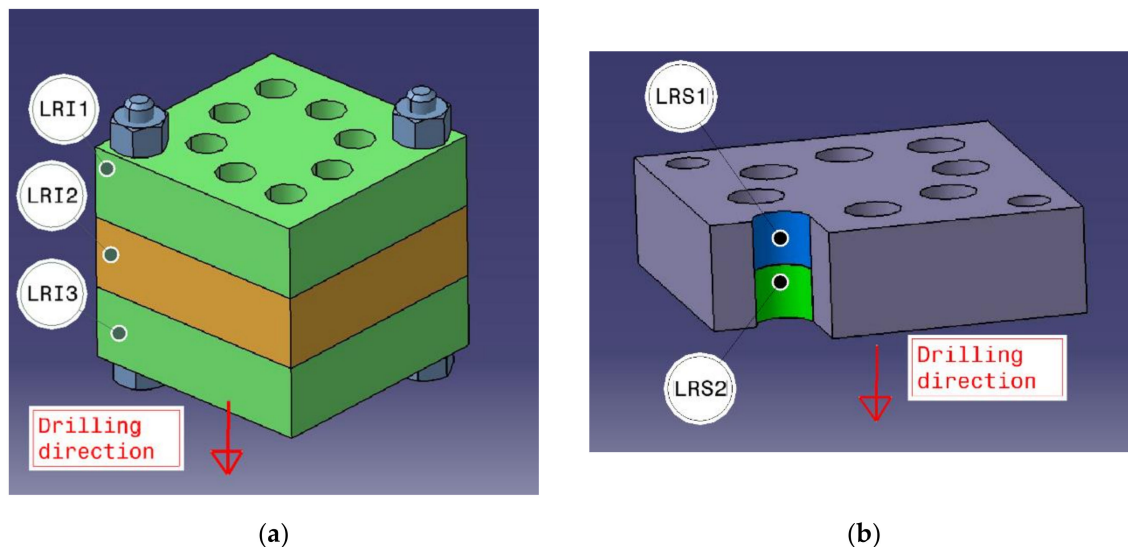


Figure 1. Detail of the position of the roughness measurements inside each Mg-Al-Mg specimen; (a) Location Regarding Insert, LRI; (b) Location Regarding Specimen, LRS.

Afterwards, machining tests were carried out. Before performing the re-drilling tests, protocols were established both for the cutting parameters and the collection of the response variable data. Subsequently, test specimens, tools, CCA equipment, and the machining center were prepared, and the selected cutting conditions introduced. Then, the machining operations were carried out. Finally, photographs were taken, and videos recorded, for subsequent analysis.

Subsequently, the response variable was measured. Specifically, the surface roughness was selected and analyzed as the Arithmetical Mean Roughness, *Ra* (μm). Once the data were collected, a statistical analysis was carried out. The variability of the *Ra* (μm) was modeled using Analysis of Variance (ANOVA), the factors, and interactions between them with an influence on surface roughness were identified. Finally, the results were statistically analyzed, and conclusions drawn.

2.2. Equipment, Tools, and Materials

The following equipment, tools, and materials were used to conduct the study:

- Tongtai TMV510 Machining center (Tongtai Machine and Tool Co, Luzhu Dist, Kaohsiung City, Taiwan) equipped with FANUC series OI-MC numerical control (FANUC Iberia, Castelldefels, Barcelona, Spain) (Figure 2a).
- Cold Compressed Air system from Cold Air Gun Vortec (Vortec, Cincinnati, Ohio, U.S.). This equipment uses vortex tube technology and filtered compressed air to produce a compressed air of a working temperature of 8 °C. The equipment employs no moving parts, does not require electricity, just a compressed air source [61]. (Figure 2b).
- Mitutoyo Surftest SJ 401 Roughness tester (Mitutoyo America Corporation, Aurora, IL, USA) (Figure 2c).
- A 9 mm diameter high performance twist drill with supplier reference HSS-E-PM-A1 1257. Supplier Garant (Hoffmann Iberia Quality Tools S.L., San Fernando de Henares, Madrid, Spain) (Figure 2d).
- Multimaterial or hybrid compound specimens for re-drilling. These specimens consist of three intercalated plates of magnesium/aluminum/magnesium alloys of 15 mm thickness. The combination of the different material layers is designed to allow the drill bit passing from one material to another during the machining of the hole. The operations performed aim to simulate the repair operations on hybrid components. For this reason, specimens used already have 8 mm pre-drilled holes, and the procedure consists of re-drilling them to a slightly larger diameter of 9 mm. The shape of each plate is a parallelepiped whose dimensions are 50 × 50 × 15 mm. The three parallelepipeds are mechanically fixed so that the surface roughness inside the machined holes can be dismantled and measured relatively easily (Figure 2e). The chemical compositions of the magnesium and aluminum alloys used are available in Table 3.



(a)



(b)



(c)



(d)

Figure 2. Cont.

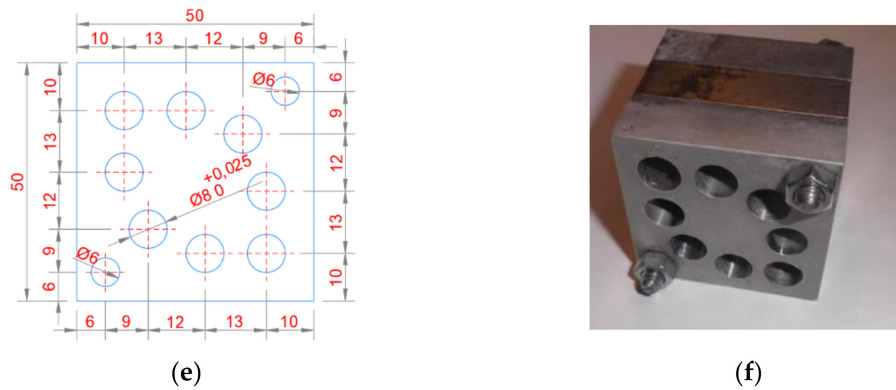


Figure 2. Main equipment, tools, and materials used during the trials. (a) Tongtai TMV510 machining center; (b) Vortec Cold Air Gun; (c) Mitutoyo SurfTest SJ 401 roughness tester; (d) helical drill bits HSS-E-PM A1 1257 manufactured by Garant; (e) overall dimensions of the re-drilling specimen; (f) specimen Mg-Al-Mg.

Table 3. Chemical composition of the materials used for the manufacturing specimens of UNS M11917 (AZ91D) and UNS A92024 (AA2024 T351).

UNS M11917 (AZ91D)	UNS A92024 (AA2024 T351)
Al 8.30–9.70%	Al 90.7–94.7%
Cu ≤ 0.03%	Cr ≤ 0.1%
Fe ≤ 0.005%	Cu 3.8–4.9%
Mg 90%	Fe ≤ 0.5%
Mn ≥ 0.13%	Mg 1.2–1.8%
Ni ≤ 0.002%	Mn 0.3–0.9%
Si ≤ 0.1%	Si ≤ 0.5%
	Ti ≤ 0.15%
Zn 0.35–1%	Zn ≤ 0.25%

A schematic diagram of the experimental configuration for re-drilling tests on Mg-Al-Mg multimaterial specimens is shown in Figure 3. The figure schematically shows the different stages of Taguchi-based research and the main materials employed. Predrilled specimens were tested using a machining center and cutting tool. Tests were carried out according to a predefined test plan in a Taguchi-based experimental design. Tests allow data collection of the response variable at each position predefined as potentially significant. Finally, this data is statistically analyzed using descriptive statistics and analysis of variance.

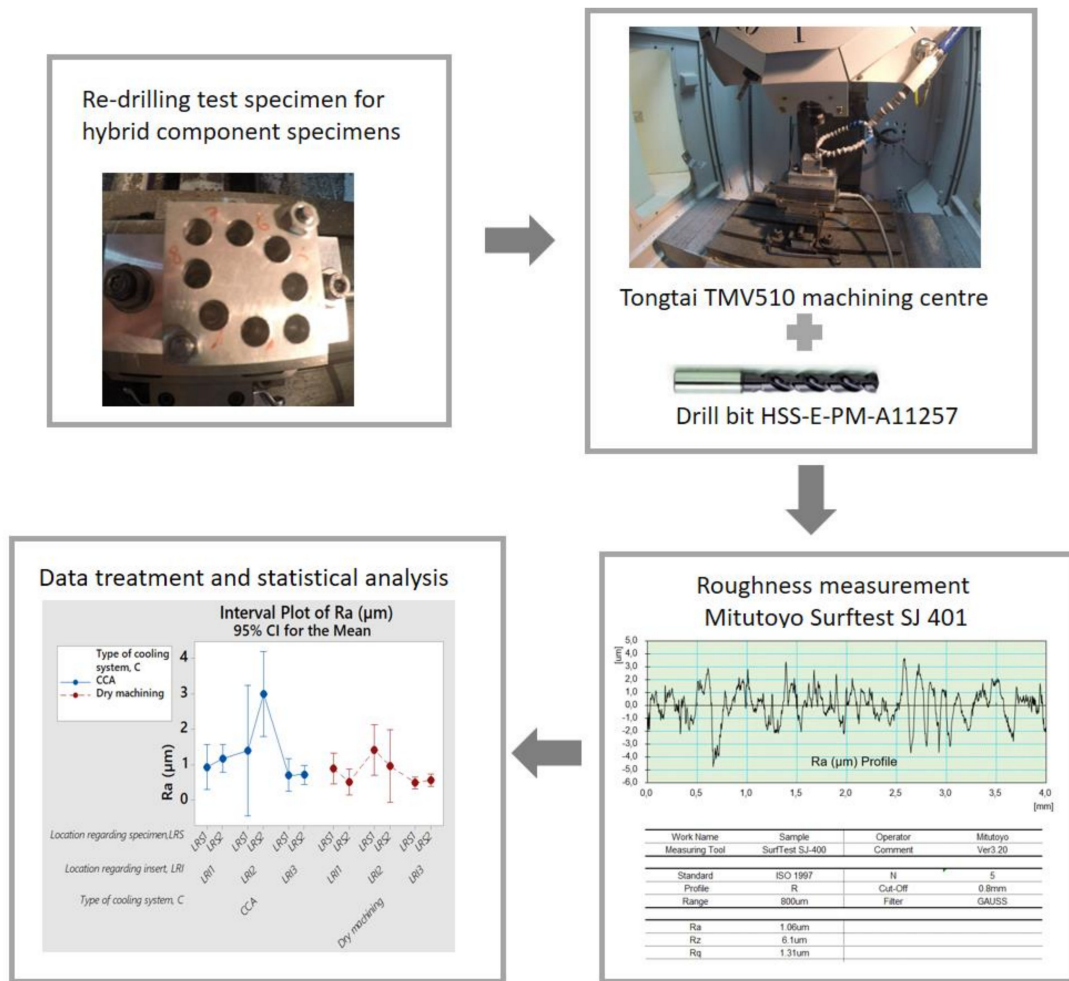


Figure 3. Schematic diagram of the experimental set-up for the re-drilling trials on Mg-Al-Mg multimaterial specimens.

3. Results, Analysis, and Discussion

3.1. Results

The details of the experiment and the measurements obtained are summarized in Table 4. The usual range of roughness tolerances required in the aeronautical and aerospace sector in terms of Ra (μm) is $0.8 \mu\text{m} < Ra < 1.6 \mu\text{m}$ [41]. Generally, each range of surface roughness is associated with a dimensional tolerance and a production cost. In other words, to achieve an optimum surface tolerance, a very accurate finishing is required and, therefore, more time will be required in the finishing operations and a better-quality tool and equipment will be needed. In short, the best finishing is associated with a higher cost of the manufacturing process.

Generally, a low surface roughness does not create problems in the case of repair and maintenance operations since the aim of a surface roughness tolerance is the limitation of corrosion and crack propagation. In operations where higher surface roughness is required, such as painting or areas where the plasma will be projected, a preblasting is carried out to increase the roughness of the surface [62–65].

Table 4. Mg-Al-Mg test. Arithmetical Mean Roughness, Ra (μm) in each plate at the entry and at the exit zones of the holes.

Test No.	1	2	3	4	5	6	7	8	AV	STD
LRI1/LRS1 Ra (μm)	0.35	1.06	1.27	1.03	1.22	0.61	0.73	0.98	0.91	0.30
LRI1/LRS2 Ra (μm)	0.81	1.23	1.31	1.33	0.19	0.73	0.48	0.62	0.84	0.39
LRI2/LRS1 Ra (μm)	2.94	1.31	1.2	0.13	1.24	1.88	0.87	1.66	1.40	0.76
LRI2/LRS2 Ra (μm)	3.00	3.95	2.11	2.91	1.30	0.51	0.33	1.70	1.98	1.18
LRI3/LRS2 Ra (μm)	0.48	0.64	0.56	1.13	0.34	0.53	0.46	0.59	0.59	0.22
LRI3/LRS2 Ra (μm)	0.59	0.56	0.78	0.92	0.67	0.63	0.42	0.53	0.64	0.15
f (mm/rev)	0.05	0.05	0.10	0.10	0.05	0.05	0.10	0.10		
N (rpm)	500	1200	500	1200	500	1200	500	1200		
Type of cooling system, C	CCA	CCA	CCA	CCA	Dry	Dry	Dry	Dry		
Av	1.36	1.46	1.21	1.24	0.83	0.82	0.55	1.01		
STD	1.15	1.15	0.49	0.84	0.45	0.48	0.19	0.49		

In Table 4, the values obtained within the required tolerance range are represented in green text, and the values below the minimum required tolerance are represented in blue text. When blue values appear, the process could be better adjusted so that all measurements remain below the maximum tolerance but optimizing the cost and time of the machining operation. Roughness measurements above the maximum tolerance are represented in red text and are not acceptable.

3.2. Analysis and Discussion

A study of the factors of significant influence, regarding the response variable Ra (μm), was performed using an analysis of variance. The analysis was completed in several steps, initially, Ra (μm) data were directly analyzed, but the values did not follow a normal distribution (Shapiro–Wilk test p -value < 0.05) so the analysis could not continue since this requirement was not met. Later, a logarithmic transformation of the data was performed, which maintained the order but smoothed out the effect of outliers (Table 5). The analysis of the transformed data did show a normal distribution of Ra (μm) (Shapiro–Wilk test p -value > 0.05), shown in Figure 4a. Then, the condition of homoscedasticity was verified (Levene Statistic, p -value > 0.05), and the independent data sets had a similar number of cases. Interactions of up to third order were considered in the analysis, and successive iterations were performed until all values were significant. In each iteration, the statistically less significant effect was excluded, in case it had a p -value higher than 0.05.

Table 5. Mg-Al-Mg test. Last ANOVA iteration for $\text{Ln}Ra$ values.

Source	Squares Sum	DF *	Mean Square	F	Sig.
Corrected model	11.496 ^a	11	1.045	3.372	0.003
Intercept	1.486	1	1.486	4.795	0.035
C	1.882	1	1.882	6.072	0.019
LRI	4.983	2	2.491	8.038	0.001
LRS	0.097	1	0.097	0.314	0.578
$C * LRI$	0.070	2	0.035	0.113	0.893
$C * LRS$	2.243	1	2.243	7.238	0.011
$LRI * LRS$	0.471	2	0.236	0.760	0.475
$C * LRI * LRS$	1.749	2	0.875	2.822	0.073
Error	11.158	36	0.310		
Total	24.141	48			
Corrected total	22.654	47			

* DF: degrees of freedom. ^a R squared = 0.507 (adjusted R squared = 0.357).

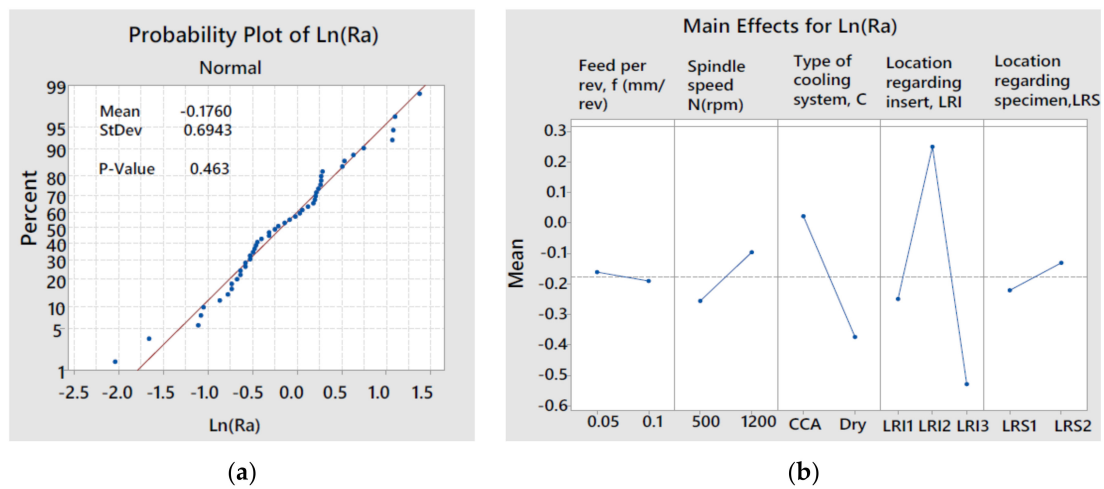


Figure 4. Mg-Al-Mg test. (a) Normality of the distribution LnRa. (b) Main effects over LnRa.

From the analysis of variance, it is concluded that the two significant factors in the process are the location regarding the insert, *LRI*, and the type of cooling system, *C*. These results are consistent with previous works [58,60] and there is also an interaction, unknown so far, between the type of cooling system, *C*, and the location regarding the specimen, *LRS*. Table 6 shows the percentage of variability attributed to each factor obtained as a percentage of the sum of squares of each significant factor with respect to the total sum of squares of the significant effects. Besides, in Figure 4b, where the effects of the different levels chosen on the factors are shown separately, it can be generally seen that lower values of *Ra* are obtained for *f* = 0.10 mm/rev, *N* = 500 rpm, under dry machining conditions, in the second magnesium plate, *LRI3*(Mg3), and in the measurement made at the hole entrance, *LRS1*.

Table 6. Mg-Al-Mg test. Percentage of variability of each factor on LnRa according to ANOVA.

Source	Squares Sum	Percentage of Variability
<i>C</i>	1.882	20.7%
<i>LRI</i>	4.983	54.7%
<i>C * LRS</i>	2.243	24.6%

Figure 5 shows a higher surface roughness at the exit of the re-drilling of the central aluminum plate, *LRS2*, than at the entrance, *LRS1*, in the case of CCA cooling, with a directional effect on the process. The effect is however the opposite, although less pronounced, in the case of dry machining. A significant interaction between the type of cooling system, *C*, and the Location Regarding the Specimen, *LRS*, was detected as well by the ANOVA analysis and summarized in Table 5.

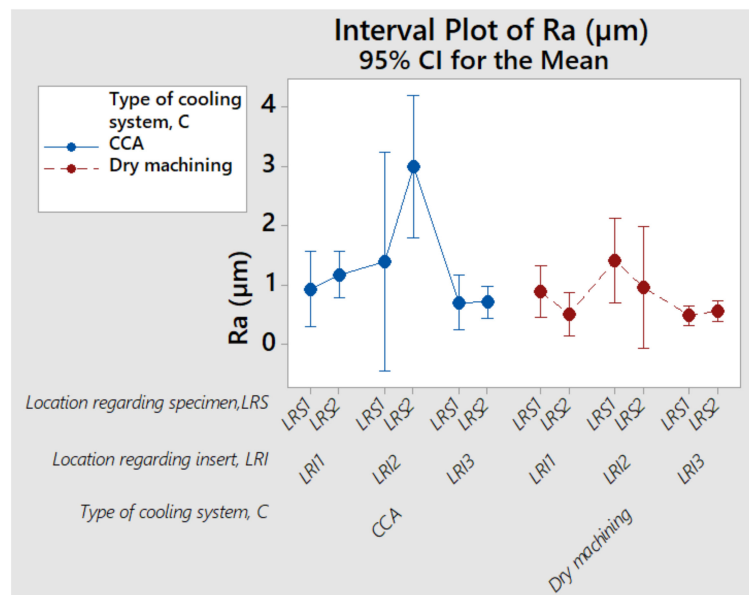


Figure 5. Mg-Al-Mg test. (a) Multiple interval plot with groups: type of cooling system type, C; Location Regarding Insert, LRI; Location Regarding Specimen, LRS.

Based on the results of the trial, the following preliminary conclusions are drawn:

- It is possible to obtain all Ra values below the maximum limits of the strict tolerances required in the aeronautical sector when repairing hybrid Mg-Al-Mg components by re-drilling using sustainable lubrication systems. Tests 5 and 7.
- The factors with a significant effect on the response variable Ra are C (20.7%), LRI (54.7%), and the interaction C * LRS (24.6%).
- Tests 2 and 3 would allow the re-drilling of 15 mm magnesium plates and 7.5 mm aluminum plates. For thicker aluminum plates, the data obtained give roughness values outside the optimum range for the aeronautical sector.
- The factor of the type of cooling system, C, has a clear significant influence on the roughness obtained in the aluminum plate and, in particular, on the output values of the re-drilling (LRI2-LRS2). In this area, by dry machining, the roughness obtained at the exit of the drill is within the range typical of the aeronautical industry (1.30 µm in test 5) or higher than those accepted, but very close (1.70 µm in test 8) while, with cold compressed air cooling, all the values obtained are out of tolerance (3.00, 3.95, 2.11, and 2.91 µm in tests 1, 2, 3, and 4, respectively).
- Based on the results, there seems to be a dependent directional effect in addition to the cooling/lubrication used, and consequently, the conduction of new tests is proposed to verify the influence of the drilling direction on the Ra , that is, if there is a significant difference in making the re-drilling of the hybrid compound starting from the magnesium plate or the aluminum plate.

These conclusions confirm and complement the factors of influence found in previous studies on Mg-Al-Mg multimaterial compounds, confirm the possibility of using sustainable machining processes in the repair of magnesium-based multimaterial compounds, provide new knowledge of the process such as the dependence of the final quality of the machining on the thickness of the plates of the multimaterial compound. This new knowledge allows to establish the basis for designing new configurations of hybrid multimaterial specimens to continue advancing in the development of sustainable machining techniques aimed at reuse after repair of magnesium-based multimaterial components, and with application in the aeronautical and/or automotive sector.

Another novelty contributed by this study is to carry out a comparative analysis regarding previous studies, giving an enriching global perspective applicable to magnesium-based multimaterials.

This comparison is possible because the studies are part of the same project and have been designed following a comparable methodology based on Taguchi [59]. Below, the data was obtained by Rubio and his collaborators [18] in the test of Mg-Ti-Mg specimens, in which the magnesium alloy is identical to the one used in this study, UNS M11917 (AZ91D) and whose composition was already shown in Table 3, and the titanium alloy is UNS R56400 (Ti-6Al-4V) whose composition is shown in Table 7.

Table 7. Chemical composition of UNS R56400 (Ti-6Al-4V) specimens.

UNS R56400 (Ti-6Al-4V)	
Al	5.5–6.75%
C	≤ 0.08%
H	≤ 0.015%
Fe	≤ 0.4%
N	≤ 0.03%
O	≤ 0.2%
Ti	87.725–91%
Zn	3.5–4.5%

Table 8 includes the experimental plan followed, Table 9 details the *Ra* obtained values in the tests, Table 10 shows the result of the analysis of variance for the obtained values, factors, and levels, and Table 11 shows the percentages of the variability of each factor according to the results of the ANOVA. Tables 8–11 were adapted from [18] following the structure defined in this work to facilitate the comparison of the results.

Table 8. Mg-Ti-Mg specimen experimental design: product of a full factorial 2³ and a block of two factors.

Test No.	1	2	3	4	5	6	7	8
<i>LRI/LRS</i>	<i>LRI1/LRS1</i>							
	<i>LRI1/LRS2</i>							
	<i>LRI2/LRS1</i>							
	<i>LRI2/LRS2</i>							
	<i>LRI3/LRS1</i>							
	<i>LRI3/LRS2</i>							
Type of tool, <i>T</i>	<i>T1</i>	<i>T1</i>	<i>T1</i>	<i>T1</i>	<i>T2</i>	<i>T2</i>	<i>T2</i>	<i>T2</i>
<i>V</i> (m/min)	<i>V1</i>	<i>V1</i>	<i>V2</i>	<i>V2</i>	<i>V1</i>	<i>V1</i>	<i>V2</i>	<i>V2</i>
Feed rate, <i>f</i> (mm/min)	<i>f2</i>	<i>f1</i>	<i>f2</i>	<i>f1</i>	<i>f2</i>	<i>f1</i>	<i>f2</i>	<i>f1</i>

Table 9. Mg-Ti-Mg test. Arithmetical Mean Roughness, *Ra* (µm), measured in each plate at the entry and at the exit zones of the holes. Adapted from [18].

Test No.	1	2	3	4	5	6	7	8	AV	STD
<i>LRI1/LRS1 Ra</i> (µm)	0.36	1.23	0.10	1.73	1.59	1.73	0.68	2.62	1.38	0.75
<i>LRI1/LRS2 Ra</i> (µm)	1.73	0.31	0.87	1.54	0.77	0.37	0.45	1.65	0.85	0.51
<i>LRI2/LRS1 Ra</i> (µm)	1.28	0.74	0.86	0.86	0.80	1.60	1.11	1.19	1.02	0.28
<i>LRI2/LRS2 Ra</i> (µm)	3.09	1.46	0.89	1.34	0.85	1.03	0.87	1.34	1.11	0.24
<i>LRI3/LRS2 Ra</i> (µm)	1.52	1.91	0.78	0.64	0.83	1.81	0.61	1.63	1.17	0.54
<i>LRI3/LRS2 Ra</i> (µm)	2.28	6.28	1.09	1.94	1.43	1.79	1.28	1.78	2.23	1.68
Type of tool, <i>T</i>	A11253	A11253	A11253	A11253	A11240	A11240	A11240	A11240		
<i>V</i> (m/min)	20	20	25	25	20	20	25	25		
Feed rate, <i>f</i> (mm/min)	50	100	50	100	50	100	50	100		
Av	1.71	1.99	0.77	1.34	1.05	1.39	0.83	1.70		
STD	0.84	1.99	0.31	0.46	0.33	0.53	0.29	0.46		

Table 10. Mg-Ti-Mg test. Last ANOVA iteration for LnRa values. Adapted from [18].

Source	Squares Sum	DF *	Mean Square	F	Sig.
Corrected model	8.487 ^a	11	0.772	2.235	0.034
Intercept	0.567	1	0.567	1.643	0.208
LRI	2.440	2	1.220	3.534	0.040
T	0.022	1	0.022	0.063	0.804
f	0.017	1	0.017	0.049	0.826
LRI * T	2.948	2	1.474	4.270	0.022
LRI * f	0.243	2	0.121	0.352	0.706
T * f	2.166	1	2.166	6.275	0.017
LRI * T * f	0.651	2	0.326	0.943	0.399
Error	12.429	36	0.345		
Total	21.483	48			
Corrected total	20.916	47			

* DF: degrees of freedom. (^a R Squared = 0.406 (Adjusted R Squared = 0.224)).

Table 11. Mg-Ti-Mg test. Percentage of variability of each factor on LnRa according to ANOVA.

Source	Squares Sum	Percentage of Variability
LRI	2.440	32.3%
LRI * T	2.948	39.0%
T * f	2.166	28.7%

Similarly, and based on the analysis of the results presented by Rubio and his collaborators in 2018 [18] (Figure 6), the following preliminary conclusions can be drawn from the analysis performed in the present study:

- It is possible to obtain all Ra (µm) values below the maximum limits of the strict tolerances demanded in the aeronautical sector for a re-drilling repair of hybrid Mg-Ti-Mg components by using sustainable lubrication systems. In particular, using the cutting parameters defined in tests 3, 5, and 7, all Ra (µm) values are below 1.6 µm.
- The factor with a significant effect on the response variable Ra (µm) is the Location Regarding Insert, LRI, (32.3%), and the interactions LRI * T (39%) and T * f (28.7%).
- The conditions of test 1 would allow the re-drilling of a hybrid compound made up of two titanium and magnesium plates, in that order, each 7.5 mm thick.
- Test 4 might re-drill together three Mg-Ti-Mg plates with thicknesses of 7.5 mm for magnesium and 15 mm for titanium, making slight adjustments to the process parameters, since the roughness values in terms of Ra (µm) for magnesium, on both plates, are close to the standard values in the aeronautical sector.

As novelties provided by the joint analysis of the present work, we can state that for the Mg-Al combination, 15 mm Mg plates and 7.5 mm Al plates are generally more suitable, whereas, for Mg-Ti combinations, 7.5 mm Mg plates and 15 mm Ti plates seem more favorable.

These conclusions make it possible to design new configurations of hybrid multimaterial specimens to obtain more information in future tests. This information will lead to better comprehension of the relationship between the quality of the final machining and the thickness of the plates of magnesium-based multimaterials, a possible directional influence on machining, and to continue progressing in the development of sustainable machining techniques applicable to magnesium-based multimaterial components in the aeronautical and/or automotive sectors. Therefore, new tests are proposed on Mg-Al-Mg and Mg-Ti-Mg specimens with the same cutting parameters in both, and a higher number of levels for each analyzed factor to verify the similarities, or not, of the results obtained.

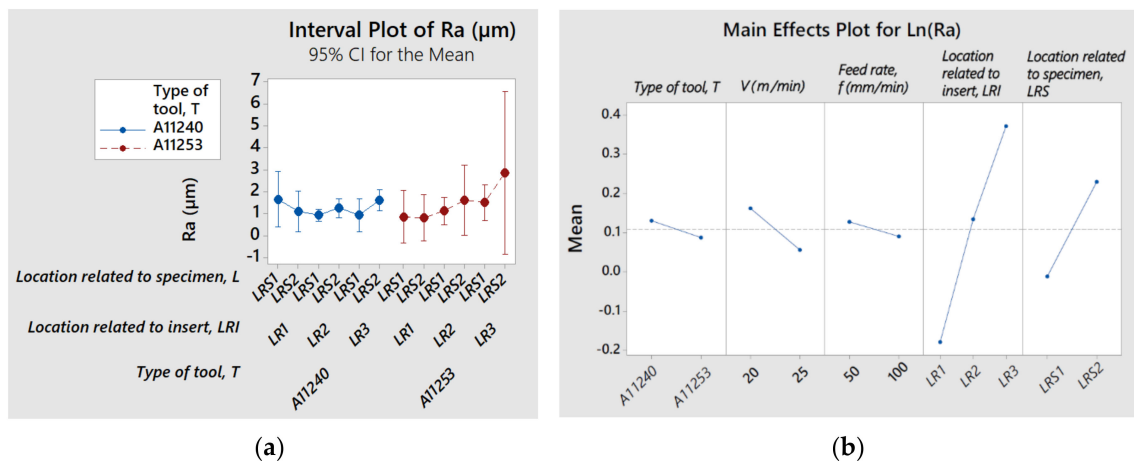


Figure 6. Mg-Ti-Mg test. (a) Multiple interval plot with groups: tool type, T , Location Regarding Insert, LRI , and Location Regarding Specimen, LRS ; (b) main effects over $\text{Ln}Ra$. Based on data from [18].

Likewise, it is proposed to redesign, manufacture, and test with similar cutting parameters new specimens of two and three plates of magnesium, aluminum, and titanium. More specifically, specimens made up of two Mg-Al and Mg-Ti plates, and of three Mg-Al-Mg and Mg-Ti-Mg plates, taking into account the results obtained in this work, mentioned above, concerning the thicknesses of the plates, which will be made with the same cutting parameters in both specimens and, regarding their dimensioning, with the values included in the European standards [66,67] and international ISO standards on rivets for aerospace application [68,69].

4. Conclusions

This study is included in a larger project that focuses on the development of sustainable machining techniques applicable to hybrid multimaterial components made of magnesium-based light alloys. As a novelty, it presents an analysis of magnesium-based multimaterial compounds focusing on the relationship between the thickness of the plates that form the compound and the multimaterial combination used, and the directionality of the process. This analysis was carried out from a joint perspective and applying the previous knowledge acquired, so that in addition to analyzing the data obtained in the individual experiment carried out for this study on a Mg-Al-Mg component, a comparative analysis was also carried out with the data obtained in a previous trial framed in the same project, and carried out on a Mg-Ti-Mg multimaterial combination. The data from both studies are comparable as they follow the same methodological structure based on Taguchi, and designed for this purpose. The data from the previous study were reanalyzed following the perspective, objectives, and structure of the present study. Specifically, the design selected was a product of a complete factorial 2^3 and a block of two factors (3×2) that includes eight re-drilling tests. The following conclusions were drawn from this experiment:

This study aimed to establish a basis for adapting or redesigning the current project specimens to allow them to be used in the study of applications involving the riveting of multimaterial plates made of light alloys in the aerospace industry, especially those made of magnesium-based alloys. To this end, the relationship between the surface quality obtained after re-drilling different combinations of magnesium-based multimaterials, the thicknesses of the plates that form them, and the cutting parameters were analyzed, all oriented towards repair and maintenance processes of parts by re-drilling in the aeronautical industry, and with the essential need to guarantee the design requirements throughout their useful life.

The following conclusions were drawn from this experiment:

- It is possible to obtain all Ra (μm) values below the maximum limits of the strict tolerances required in the aeronautical sector for the repair by re-drilling of hybrid Mg-Al-Mg components through sustainable lubrication systems. Tests 5 and 7.
- The factors with a significant effect on the response variable Ra (μm) are the type of cooling system, C (20.7%), the Location Regarding Insert, LRI (54.7%), and the interaction between the type of cooling system * Location Regarding Specimen, $C * LRS$ (24.6%).
- Tests 2 and 3 would allow the re-drilling of 15 mm magnesium plates and 7.5 mm aluminum plates. For thicker aluminum sheets, however, the data obtained give values of roughness outside the optimal range for the aeronautical sector.
- Factor type of cooling system, C , has a clear effect on the roughness obtained on the aluminum plate, since, whereas with dry machining, the values obtained are within the tolerance for the plate of 15 mm (1.24 and 1.30 in test 4) or relatively close to the standard values (1.66 and 1.7 μm in test 8), with Cold Compressed Air cooling all the exit values of the aluminum plate are out of tolerance (2.11, 2.91, 3.00, and 3.95 μm); therefore, using this cooling system, the intermediate plate could not be thicker than 7.5 mm.
- Based on the results, there seems to be a dependent directional effect in addition to the cooling/lubrication used, and consequently, it is proposed the conduction of new tests to verify the influence of the drilling direction on the Ra , that is, if there is a significant difference in making the re-drilling of the hybrid compound starting from the magnesium plate or the aluminum plate.
- On the other hand, the results of this study were analyzed and compared with those obtained in a previous study on an Mg-Ti-Mg specimen with similar geometric characteristics, concluding that, for the Mg-Al combination, 15 mm Mg and 7.5 mm Al plates are generally more suitable, while, for Mg-Ti, 7.5 mm Mg and 15 mm Ti plates seem more suitable when creating the hybrid compounds.

Author Contributions: E.M.R., M.M.M. and D.B. contributed to the conceptualization, methodology, and formal analysis. D.B. performed the investigation. E.M.R. and M.M.M. managed the project resources. E.M.R., M.M.M. and D.B. prepared the original draft of the manuscript. E.M.R., M.M.M., D.B. and J.M.S.d.P. reviewed and edited the manuscript. E.M.R., M.M.M., D.B. and J.M.S.d.P. contributed to data visualization. E.M.R., M.M.M., and J.M.S.d.P. supervised the study. E.M.R. and M.M.M. were responsible for the funding acquisition and project administration. All authors have read and agreed to the published version of the manuscript.

Funding: This work was partly funded by grants from the Ministerio de Ciencia, Innovación, y Universidades, and the Industrial Engineering School-UNED (RTI2018-102215-B-I00, REF 2020-ICF04 y REF2020-ICF07), Spain.

Acknowledgments: The authors thank the Industrial Production and Manufacturing Engineering (IPME) Research Group and the Industrial Engineering School-UNED (REF 2020-ICF04 y REF2020-ICF07).

Conflicts of Interest: The authors declare no conflict of interest.

References

1. Advisory Council for Aeronautics Research in Europe (ACARE). Available online: <https://www.acare4europe.org/sria/flightpath-2050-goals/protecting-environment-and-energy-supply-0> (accessed on 14 August 2020).
2. Global Market Forecast 2019–2038 Airbus Commercial Aircraft Book. Available online: <https://www.airbus.com/content/dam/corporate-topics/strategy/global-market-forecast/GMF-2019-2038-Airbus-Commercial-Aircraft-book.pdf> (accessed on 15 August 2020).
3. ICAO. Effects of COVID-19 on Civil Aviation: Economic Impact Analysis. Available online: https://www.icao.int/sustainability/Documents/COVID-19/ICAO_Coronavirus_Econ_Impact.pdf (accessed on 8 November 2020).
4. Airbus Plans to Further Adapt to COVID-19 Environment. Available online: <https://www.airbus.com/newsroom/press-releases/en/2020/06/airbus-plans-to-further-adapt-to-covid19-environment.html> (accessed on 8 November 2020).

5. Boeing Forecasts Challenging Near-Term Aerospace Market with Resilience in Long Term. Available online: <https://boeing.mediaroom.com/2020-10-06-Boeing-Forecasts-Challenging-Near-Term-Aerospace-Market-with-Resilience-in-Long-Term> (accessed on 8 November 2020).
6. Airbus Reports Nine-Month (9m) 2020 Results. Available online: <https://www.airbus.com/newsroom/press-releases/en/2020/10/airbus-reports-nine-month-9m-2020-results.html> (accessed on 8 November 2020).
7. Karpat, Y.; Deger, B.; Bahtiyar, O. Drilling thick fabric woven CFRP laminates with double point angle drills. *J. Mater. Process. Technol.* **2012**. [[CrossRef](#)]
8. International Council on Clean Transportation (ICCT). Available online: <https://theicct.org/aviation> (accessed on 14 August 2020).
9. Walker, J.C.; Kamps, T.J.; Wood, R.J.K. The influence of start-stop transient velocity on the friction and wear behaviour of a hyper-eutectic Al-Si automotive alloy. *Wear* **2012**, *306*, 209–218. [[CrossRef](#)]
10. European Commission. Renewable Energy Directive. Available online: https://ec.europa.eu/energy/topics/renewable-energy/renewable-energy-directive/overview_en (accessed on 8 November 2020).
11. 2020 Boeing Global Environment Report. Available online: <http://www.boeing.com/principles/environment/index.page> (accessed on 7 September 2020).
12. Airbus Environment. Available online: <https://www.airbus.com/content/dam/corporate-topics/corporate-social-responsibility/environment/Environment-matters-for-the-future-of-aerospace.pdf> (accessed on 9 May 2020).
13. 2018 Boeing Global Environmental Report. Available online: https://s2.q4cdn.com/661678649/files/doc_downloads/env_reports/2018_environment_report.pdf (accessed on 2 September 2020).
14. Kulkarni, S.; Edwards, D.J.; Parn, E.A.; Chapman, C.; Aigbavboa, C.O.; Cornish, R. Evaluation of vehicle lightweighting to reduce greenhouse gas emissions with focus on magnesium substitution. *J. Eng. Des. Technol.* **2018**, *16*, 869–888. [[CrossRef](#)]
15. Uhlmann, E.; Kersting, R.; Klein, T.B.; Cruz, M.F.; Borille, A.V. Additive Manufacturing of Titanium Alloy for Aircraft Components. *Procedia CIRP* **2015**, *35*, 55–60. [[CrossRef](#)]
16. Ezugwu, E.O. High speed machining of aero-engine alloys. *J. Braz. Soc. Mech. Sci. Eng.* **2004**, *26*, 1–11. [[CrossRef](#)]
17. Li, D.; Chrysanthou, A.; Patel, I.; Williams, G. Self-piercing riveting—A review. *Int. J. Adv. Manuf. Technol.* **2017**, *92*, 1777–1824. [[CrossRef](#)]
18. Maria Rubio, E.; Villeta, M.; Luis Valencia, J.; de Pipaon, J. Cutting Cutting parameter selection for efficient and sustainable repair of holes made in hybrid Mg-Ti-Mg component stacks by dry drilling operations. *Materials* **2018**, *11*, 1369. [[CrossRef](#)]
19. Rubio, E.M.; Villeta, M.; Valencia, J.L.; de Pipaón, J.M.S. Experimental study for improving the repair of magnesium-aluminium hybrid parts by turning processes. *Metals* **2018**, *8*, 59. [[CrossRef](#)]
20. Berzosa, F.; de Agustina, B.; Rubio, E.M. Tool Selection in Drilling of Magnesium UNSM1917 Pieces under Dry and MQL Conditions Based on Surface Roughness. *Procedia Eng.* **2017**, *184*, 117–127. [[CrossRef](#)]
21. Rubio, E.M.; Blanco, D.; Marín, M.M.; Carou, D. Analysis of the latest trends in hybrid components of lightweight materials for structural uses. *Procedia Manuf.* **2019**, *41*, 1047–1054. [[CrossRef](#)]
22. Blanco, D.; Rubio, E.M.; Marín, M.M.; Davim, J.P. Advanced materials and multi-materials applied in aeronautical and automotive fields: A systematic review approach. In Proceedings of the 14th CIRP Conference on Intelligent Computation in Manufacturing Engineering, Gulf Naples, Italy, 15–18 July 2020.
23. Manakari, V.; Parande, G.; Gupta, M. Selective Laser Melting of Magnesium and Magnesium Alloy Powders: A Review. *Metals* **2016**, *7*, 2. [[CrossRef](#)]
24. Weltsch, Z. Comparative study of the joining technologies of vehicle bodywork sheets. *IOP Conf. Ser. Mater. Sci. Eng.* **2018**, *448*, 012061. [[CrossRef](#)]
25. Airbus, Product Responsibility. Available online: <https://www.airbus.com/company/sustainability/environment/product-responsibility.html> (accessed on 14 May 2020).
26. Aamir, M.; Giasin, K.; Tolouei-Rad, M.; Vafadar, A. A review: Drilling performance and hole quality of aluminium alloys for aerospace applications. *J. Mater. Res. Technol.* **2020**, *9*. [[CrossRef](#)]
27. The Aluminum Association. Recycling. Available online: <https://www.aluminum.org/industries/production/recycling> (accessed on 5 November 2020).
28. International Magnesium Association. Recycling Magnesium. Available online: https://www.intlmag.org/page/sustain_recycle_ima (accessed on 5 November 2020).

29. Sáenz de Pipaón, J.M. Diseño y Fabricación de Probetas de Componentes Híbridos con Aleaciones de Magnesio Para Ensayos de Mecanizado. Ph.D. Thesis, UNED, Madrid, Spain, 2013.
30. Nguyen, H.; Zatar, W.; Mutsuyoshi, H. Hybrid polymer composites for structural applications. In *Hybrid Polymer Composite Materials*; Elsevier: Amsterdam, The Netherlands, 2017; pp. 35–51.
31. Kim, Y.-W.; Kim, S.-L. Advances in Gammalloy Materials-Processes-Application Technology: Successes, Dilemmas, and Future. *JOM* **2018**, *70*, 553–560. [[CrossRef](#)]
32. Elahinia, M.; Moghaddam, N.S.; Andani, M.T.; Amerinatanzi, A.; Bimber, B.A.; Hamilton, R.F. Fabrication of NiTi through additive manufacturing: A review. *Prog. Mater. Sci.* **2016**, *83*, 630–663. [[CrossRef](#)]
33. Xu, J.; Mkaddem, A.; El Mansori, M. Recent advances in drilling hybrid FRP/Ti composite: A state-of-the-art review. *Compos. Struct.* **2016**, *135*, 316–338. [[CrossRef](#)]
34. Haghshenas, M.; Gerlich, A.P. Joining of automotive sheet materials by friction-based welding methods: A review. *Eng. Sci. Technol. Int. J. JESTECH* **2018**, *21*, 130–148. [[CrossRef](#)]
35. Cirillo, P.; Marino, A.; Natale, C.; Di Marino, E.; Chiacchio, P.; De Maria, G. A low-cost and flexible solution for one-shot cooperative robotic drilling of aeronautic stack materials. *IFAC Pap.* **2017**, *50*, 4602–4609. [[CrossRef](#)]
36. Aamir, M.; Tolouei-Rad, M.; Giasin, K.; Nosrati, A. Recent advances in drilling of carbon fiber-reinforced polymers for aerospace applications: A review. *Int. J. Adv. Manuf. Technol.* **2019**, *105*. [[CrossRef](#)]
37. Karpat, Y.; Bahtiyar, O. Comparative Analysis of PCD Drill Designs During Drilling of CFRP Laminates. *Procedia CIRP* **2015**, *31*, 316–321. [[CrossRef](#)]
38. Díaz-Álvarez, A.; Díaz-Álvarez, J.; Santiuste, C.; Miguélez, M.H. Experimental and numerical analysis of the influence of drill point angle when drilling biocomposites. *Compos. Struct.* **2019**, *209*. [[CrossRef](#)]
39. Aamir, M.; Tolouei-Rad, M.; Giasin, K.; Vafadar, A. Feasibility of tool configuration and the effect of tool material, and tool geometry in multi-hole simultaneous drilling of Al2024. *Int. J. Adv. Manuf. Technol.* **2020**, *111*, 861–879. [[CrossRef](#)]
40. Bermudo, C.; Trujillo, F.J.; Herrera, M.; Sevilla, L. Parametric analysis of the Ultimate Tensile Strength in dry machining of UNS A97075 Alloy. *Procedia Manuf.* **2017**, *13*, 81–88. [[CrossRef](#)]
41. The American Society of Mechanical Engineers. *Surface Texture: Surface Roughness, Waviness and Lay*; ANSI/ASME B46.1-2009; ASME: New York, NY, USA, 2010.
42. Flight Mechanic. Hole Repair and Hole Repair Hardware. Available online: <https://www.flight-mechanic.com/hole-repair-and-hole-repair-hardware/> (accessed on 16 August 2020).
43. Federal Aviation Administration; United States Department of Transportation. Aircraft Metal Structural Repair. In *Aviation Maintenance Technician Handbook-Airframe, Volume 1*; Mepcount Media LLC: Cheyenne, WY, USA, 2012.
44. Barry, N.; Hainsworth, S.V.; Fitzpatrick, M.E. Effect of shot peening on the fatigue behaviour of cast magnesium A8. *Mater. Sci. Eng. A* **2009**. [[CrossRef](#)]
45. Gomez-Parra, A.; Sanz, A.; Gamez, A.J. Evaluation of the functional performance in turned workpieces: Methodology and application to UNS A92024-T3. *Materials* **2018**, *11*, 1264. [[CrossRef](#)]
46. Sun, Y.; Huang, B.; Puleo, D.A.; Jawahir, I.S. Enhanced Machinability of Ti-5553 Alloy from Cryogenic Machining: Comparison with MQL and Flood-cooled Machining and Modeling. *Procedia CIRP* **2015**, *31*, 477–482. [[CrossRef](#)]
47. Pereira, O.; Celaya, A.; Urbikain, G.; Rodríguez, A.; Fernández-Valdivielso, A.; de Lacalle, L.N.L. CO₂ cryogenic milling of Inconel 718: Cutting forces and tool wear. *J. Mater. Res. Technol.* **2020**, *9*, 8459–8468. [[CrossRef](#)]
48. Suhaimi, M.A.; Yang, G.-D.; Park, K.-H.; Hisam, M.J.; Sharif, S.; Kim, D.-W. Effect of Cryogenic Machining for Titanium Alloy Based on Indirect, Internal and External Spray System. *Procedia Manuf.* **2018**, *17*, 158–165. [[CrossRef](#)]
49. Pereira, O.; Urbikain, G.; Rodríguez, A.; Fernández-Valdivielso, A.; Calleja, A.; Ayesta, I.; de Lacalle, L.N.L. Internal cryolubrication approach for Inconel 718 milling. *Procedia Manuf.* **2017**, *13*, 89–93. [[CrossRef](#)]
50. Damir, A.; Shi, B.; Attia, M.H. Flow characteristics of optimized hybrid cryogenic-minimum quantity lubrication cooling in machining of aerospace materials. *CIRP Ann. Technol.* **2019**, *68*, 77–80. [[CrossRef](#)]
51. Talla, G.; Sahoo, D.K.; Gangopadhyay, S.; Biswas, C.K. Modeling and multi-objective optimization of powder mixed electric discharge machining process of aluminum/alumina metal matrix composite. *Eng. Sci. Technol. Int. J. JESTECH* **2015**, *18*, 369–373. [[CrossRef](#)]

52. Dimitrov, D.; Uheida, E.; Oosthuizen, G.; Blaine, D.; Laubscher, R.; Sterzing, A.; Blau, P.; Gerber, W.; Damm, O.F.R.A. Manufacturing of high added value titanium components. A South African perspective. *IOP Conf. Ser. Mater. Sci. Eng.* **2018**, *430*, 012009. [CrossRef]
53. Salama, A.; Li, L.; Mativenga, P.; Whitehead, D. TEA CO₂ laser machining of CFRP composite. *Appl. Phys. A-Materials Sci. Process.* **2016**, *122*. [CrossRef]
54. Sorrentino, L.; Turchetta, S.; Colella, L.; Bellini, C. Analysis of Thermal Damage in FRP Drilling. *Procedia Eng.* **2016**, *167*, 206–215. [CrossRef]
55. Kumar, M.S.; Prabukarthi, A.; Krishnaraj, V. Study on tool wear and chip formation during drilling carbon fiber reinforced polymer (CFRP)/titanium alloy (Ti6Al4V) stacks. *Procedia Eng.* **2013**, *64*, 582–592.
56. Álvarez-Alcón, M.; López de Lacalle, L.N.; Fernández-Zacarias, F. Multiple Sensor Monitoring of CFRP Drilling to Define Cutting Parameters Sensitivity on Surface Roughness, Cylindricity and Diameter. *Materials* **2020**, *13*, 2796. [CrossRef]
57. Alvir, E.M.R.; Sáenz de Pipaón, J.M.; Villeta, M.; Valencia, J.L. Design, manufacturing, and machining trials of magnesium-based hybrid parts. In *Machining of Light Alloys*; CRC Press: Boca Raton, FL, USA, 2018; pp. 73–124.
58. Rubio, E.M.; Blanco, D.; Marín, M.M.; de Pipaón, J.M.S. Analysis of the surface roughness of Mg-Al-Mg hybrid components obtained by drilling using different cooling systems. *Procedia CIRP* **2020**. [CrossRef]
59. Montgomery, D. *Design and Analysis of Experiments*; John Wiley Sons, Inc.: New York, NY, USA, 2005.
60. Blanco, D.; Rubio, E.M.; Marín, M.M.; Davim, J.P. Repairing hybrid Mg-Al-Mg components using sustainable cooling systems. *Materials* **2020**, *13*, 393. [CrossRef]
61. VORTEC. Innovative Compressed Air Technologies. Cold Air Guns. Available online: <https://www.vortec.com/cold-air-guns> (accessed on 13 November 2020).
62. Varacalle, D.J.; Guillen, D.P.; Deason, D.M.; Rhodaberger, W.; Sampson, E. Effect of Grit-Blasting on Substrate Roughness and Coating Adhesion. *J. Therm. Spray Technol.* **2006**, *15*, 348–355. [CrossRef]
63. Rosler. Aero Engine/Airframe Preparation and Finishing. Available online: https://uk.rosler.com/fileadmin/Files/Prospekte/Aerospace/UK_EN_Aeroengine_GB_181.pdf (accessed on 5 November 2020).
64. Fauchais, P.L.; Heberlein, J.V.R.; Boulos, M.I. *Thermal Spray Fundamentals*; Springer US: Boston, MA, USA, 2014; ISBN 978-0-387-28319-7.
65. Sen, D.; Chavan, N.M.; Rao, D.S.; Sundararajan, G. Influence of Grit Blasting on the Roughness and the Bond Strength of Detonation Sprayed Coating. *J. Therm. Spray Technol.* **2010**, *19*, 805–815. [CrossRef]
66. EN 2309:1989. *Aerospace Series—Hole Sizes for Solid Rivets*; European Committee for Standardization: Brussels, Belgium, 1989.
67. EN 2149:1996. *Aerospace Series—Rivets, Solid, Universal Head, in Aluminium Alloy 5056A, Anodized or Chromated, Inch Based Series*; European Committee for Standardization: Brussels, Belgium, 1996.
68. ISO 14588:2000. *Blind Rivets—Terminology and Definitions*; International Organization for Standardization: Geneva, Switzerland, 2000.
69. ISO 15973:2000. *Closed End Blind Rivets with Break Pull Mandrel and Protruding Head—AlA/St*; International Organization for Standardization: Geneva, Switzerland, 2000.

Publisher’s Note: MDPI stays neutral with regard to jurisdictional claims in published maps and institutional affiliations.



© 2020 by the authors. Licensee MDPI, Basel, Switzerland. This article is an open access article distributed under the terms and conditions of the Creative Commons Attribution (CC BY) license (<http://creativecommons.org/licenses/by/4.0/>).